Zero-voltage nondegenerate parametric mode in Josephson tunnel junctions

Pedersen, Niels Falsig

Published in:
Journal of Applied Physics

Link to article, DOI:
10.1063/1.322636

Publication date:
1976

Document Version
Publisher's PDF, also known as Version of record

Zero-voltage nondegenerate parametric mode in Josephson tunnel junctions

N. F. Pedersen

Physics Laboratory I, The Technical University of Denmark, DK-2800 Lyngby, Denmark
(Received 8 April 1975)

A new parametric mode in a Josephson tunnel junction biased in the zero-voltage mode is suggested. It is a nondegenerate parametric excitation where the junction plasma resonance represents the input circuit, and a junction geometrical resonance represents the idler circuit. This nondegenerate mode has been observed in analog experiments. In a real junction the realization of this mode of operation depends on the coupling between the plasma resonance and the geometrical resonance, and it is argued that without an external dc magnetic field the even geometrical resonances are most favorable for such a coupling.

PACS numbers: 74.30.M, 84.30.D, 85.25.

I. INTRODUCTION

A number of authors[1-10] have investigated parametric effects in Josephson junctions, the underlying reason being its potential as a high-frequency nonlinear element. Briefly, two different schemes for parametric effects have been considered: in one the junction is biased at a finite voltage[1-5] and the Josephson oscillation is used as the pump source, in the other scheme the junction is biased at zero voltage[6-10] with a bias current $I_{dc} < I_0$ (I_0 is the maximum supercurrent), and an external pump is used. For the latter case the singly[6] and the doubly[7] degenerate modes have been discussed earlier. In the singly degenerate mode the pump frequency is at twice the junction plasma frequency; this mode has been observed indirectly in tunnel junction experiments at X-band frequencies.[8,9] In the doubly degenerate mode the pump frequency is close to the plasma frequency itself. An amplifier based on this principle, where the nonlinear element was an array of superconducting microbridges, has been reported recently.[10] In this paper a zero-voltage nondegenerate parametric mode employing the junction plasma resonance ω_p as the input circuit and the junction geometrical resonance ω_R as the idler circuit is discussed. The external pump is at the frequency $\omega_{pump} = \omega_p + \omega_R$. In the derivation, an admittance matrix approach similar to the one normally used in connection with varactor diode amplifiers will be used.

The paper is organized along the following lines: In Sec. II the zero-voltage nondegenerate parametric mode is derived; in Sec. III the result is compared to analog experiments; and in Sec. IV the possibility for observation of the effect in a real junction experiment is discussed.

II. THE ZERO-VOLTAGE NONDEGENERATE PARAMETRIC MODE

The nondegenerate parametric mode behaves differently from the singly degenerate mode with respect to two important properties. First, for the singly degenerate amplifier ($\omega_{pump} \sim 2\omega_{signal}$) the gain depends on the relative phase between the pump and the signal,[11] whereas for the nondegenerate amplifier the gain is independent of the relative phases. Second, the two modes are different with respect to noise properties,[11] and which one is preferable depends on the particular application. The singly degenerate amplifier[6] includes one resonant circuit, tuned to the signal frequency ω_s. The nondegenerate amplifier, to be discussed here (the lower sideband up-converter[11]) includes a second resonant circuit, the idler circuit, with resonance frequency $\omega_i > \omega_s$.

A junction equivalent circuit model with two resonance frequencies is shown in Fig. 1. It consists of a Josephson element satisfying the usual Josephson equations

$$I = I_0 \sin\phi, \tag{1}$$

$$\frac{d\phi}{dt} = \frac{2e}{\hbar} V, \tag{2}$$

where ϕ is the phase difference, V is the voltage across the junction, and I_0 is the maximum supercurrent. The Josephson element is shunted by a constant resistor R, a capacitor C, and by a series resonant circuit with inductance L_0, resistance r, and capacitance C. In a thin-film tunnel junction the series inductance L_0 arises from the imaginary part of the film surface impedance, which together with the capacitance C, gives rise to the geometrical resonance, ω_R.

In the following the real part of the surface impedance r will be neglected since it can be made small[12] by lowering the temperature. When the junction is biased in the zero-voltage mode ($I_{dc} < I_0$), the Josephson element may be represented by an ideal inductance[7] L_1 defined by

$$\frac{1}{L_1} = \frac{2eI_0}{\hbar} \cos\phi_0 \tag{3}$$

as shown in Fig. 1. Here $\sin\phi_0 = I_{dc}/I_0$.

The assumed equivalent circuit is only an approximate representation of the real tunnel junction. The

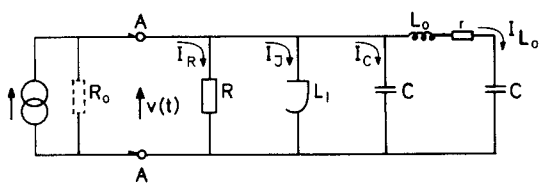

FIG. 1. Josephson junction model with a series resonant circuit.

approximations inherent in the circuit model will be discussed further in Sec. IV.

The two resonance frequencies of Fig. 1 are given by

$$\omega_1^2=\frac{2L_1+L_0}{2L_1L_0C}-\frac{(4L_1^2+L_0^2)^{1/2}}{2L_1L_0C},$$
$$\omega_2^2=\frac{2L_1+L_0}{2L_1L_0C}+\frac{(4L_1^2+L_0^2)^{1/2}}{2L_1L_0C}. \tag{4}$$

In the limit $L_0\to 0$ the resonance frequency is the plasma frequency $\omega_p=(2CL_1)^{-1/2}$, and in the limit $L_1\to\infty$ the resonance frequency is the geometrical resonance frequency $\omega_R=(2/L_0C)^{1/2}$. Assuming $L_0\ll L_1$, that is, $\omega_R\gg\omega_p$, we find that the resonance requencies of Eq. (4) are close to ω_p and ω_R. An expansion of Eq. (4) for $\omega_p/\omega_R\ll 1$ gives

$$\omega_1\sim\omega_p\left(1-\frac{1}{2}\frac{\omega_p^2}{\omega_R^2}\right),$$
$$\omega_2\sim\omega_R\left(1+\frac{1}{2}\frac{\omega_p^2}{\omega_R^2}\right). \tag{5}$$

For the circuit, Fig. 1, we now assume that the junction voltage has the form[13]

$$V(t)=V_p\cos(\omega_{pump}t)+\mathrm{Re}[V_1\exp(j\omega_1t)+V_2\exp(j\omega_2t)], \tag{6}$$

where

$$V_p\gg|V_1|,\ |V_2|, \tag{7}$$

and

$$\omega_{pump}=\omega_1+\omega_2. \tag{8}$$

The notation in Eq. (6) implies that the phases of V_1 and V_2 are measured relative to the phase of the pump signal. By integrating Eq. (2), using Eq. (6), and inserting ϕ in Eq. (1), a first-order expansion in the small quantities V_1 and V_2 by means of the Fourier–Bessel theorem[14] gives components of the supercurrent I_{1J} and I_{2J}^* at frequencies ω_1 and ω_2, respectively,

$$\begin{Bmatrix}I_{1J}\\ I_{2J}^*\end{Bmatrix}=\begin{Bmatrix}Y_{11} & Y_{12}^*\\ Y_{21} & Y_{22}^*\end{Bmatrix}\begin{Bmatrix}V_1\\ V_2^*\end{Bmatrix}, \tag{9}$$

where

$$Y_{11}=\frac{1}{j}\frac{2eI_0J_0(\alpha)}{\hbar\omega_1}\cos\phi_0,\quad Y_{12}^*=-\frac{2eI_0J_1(\alpha)}{\hbar\omega_2}\sin\phi_0,$$
$$Y_{21}=\frac{2eI_0J_1(\alpha)}{\hbar\omega_1}\sin\phi_0,\quad Y_{22}^*=-\frac{1}{j}\frac{2eI_0J_0(\alpha)}{\hbar\omega_2}\cos\phi_0. \tag{10}$$

Here $J_n(\alpha)$ is the nth-order Bessel function of argument $\alpha=2eV_p/\hbar\omega_{pump}$. The elements Y_{11} and Y_{22}^* corresponds to the inductor L_1 in Fig. 1 and Y_{12}^* and Y_{21} represents lower sideband mixing products at frequencies $\omega_{pump}-\omega_2=\omega_1$ and $\omega_{pump}-\omega_1=\omega_2$, respectively. It is observed[7] from Eq. (9) that the off-diagonal coupling strength is a function of the pump amplitude V_p.

Referring the currents to the outside of the junction (left of AA in Fig. 1) we have

$$I=I_R+I_J+I_C+I_{L_0},$$

where I_R, I_C, and I_{L_0} contributes only to the diagonal elements when added to I_J, Eq. (9). Further, since the circuit is resonant at frequencies ω_1 and ω_2 the imaginary part of the diagonal elements vanishes and we obtain for the total current to the junction I_1 and I_2^* at frequencies ω_1 and ω_2

$$\begin{Bmatrix}I_1\\ I_2^*\end{Bmatrix}=\begin{Bmatrix}1/R & Y_{12}^*\\ Y_{21} & 1/R\end{Bmatrix}\begin{Bmatrix}V_1\\ V_2^*\end{Bmatrix}, \tag{11}$$

where Y_{12}^* and Y_{21} are given by Eq. (9).

If there is no external source at the frequency ω_2 we obtain

$$I_2^*=-V_2^*/R_0, \tag{12}$$

where R_0 is the waveguide impedance (or free-space impedance) at the frequency ω_2. Combining Eqs. (11) and (12) we find the current I_1 at the frequency ω_1 to be

$$I_1=\frac{V_1}{R}-\frac{Y_{12}^*Y_{21}}{1/R+1/R_0}V_1. \tag{13}$$

Since R_0 is typically much greater than R we may substitute $1/R$ for $1/R+1/R_0$ and we find for the input admittance at frequency ω_1

$$Y_{in}(\omega_1)=\frac{I_1}{V_1}=\frac{1}{R}\left(1-\frac{[(2eI_0/\hbar)\sin\phi_0J_1(\alpha)R]^2}{\omega_1\omega_2}\right), \tag{14}$$

where Y_{12}^* and Y_{21} have been inserted from Eq. (9). Inserting[6] $Q=\omega_pRC$, $J_1(\alpha)\sim\frac{1}{2}\alpha$, and using $\omega_1\sim\omega_p$ and $\omega_2\sim\omega_R$ [Eq. (5)] we may approximate Eq. (14);

$$Y_{in}(\omega_p)\approx\frac{1}{R}\left[1-\frac{\omega_p}{\omega_R}\left(\frac{\alpha\tan\phi_0}{2/Q}\right)^2\right]. \tag{15}$$

The input admittance at the plasma resonance becomes negative when the threshold condition

$$\alpha\tan\phi_0>\left(\frac{\omega_R}{\omega_p}\right)^{1/2}\frac{2}{Q} \tag{16}$$

is satisfied.

For the singly degenerate mode ($\omega_{pump}\approx 2\omega_p$) the input admittance at the plasma frequency may be shown to be

$$Y_{in}(\omega_p)\approx\frac{1}{R}\left(1-\frac{\alpha\tan\phi_0}{2/Q}\exp(-j\theta_s)\right) \tag{17}$$

with a threshold condition[6] for parametric oscillations

$$\alpha\tan\phi_0>2/Q; \tag{18}$$

here θ_s is the phase of the signal voltage relative to the pump voltage.

When comparing Eqs. (16) and (18) we note that the threshold pump power has been raised in the nondegenerate mode; however, as can be seen from Eqs. (15) and (17) the phase dependence has disaapeared. Also the noise temperature of the nondegenerate mode has been reduced compared to the singly degenerate mode since it is proportional to ω_p/ω_R.[11] It is noted that the formalism used here is the same as the one commonly used for varactor diode parametric amplifiers. Hence, once the negative input admittance is derived, formulas for gain, bandwidth, noise temperature, etc., may be found in standard textbooks[11] with suitable substitutions[15] changing the nonlinear series capacitance of the varactor to a nonlinear parallel inductance.

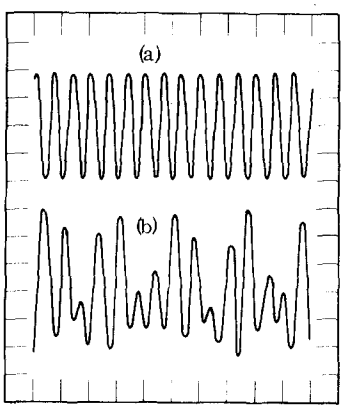

FIG. 2. Voltage waveforms (a) just below threshold, (b) just above threshold. Scale: horizontal axis, 50 μs/div; vertical axis, 50 mV/div. $f_{pump} = 34.4$ kHz, $f_p = 9.4$ kHz, and $f_R = 25$ kHz. Circuit parameters are in the text.

III. ANALOG EXPERIMENTS

The preceding calculations were compared to corresponding analog measurements. The analog has been described elsewhere[16] and has an equivalent diagram similar to Fig. 1 with the following parameters: $I_0 = 1$ mA, $k = 2e/h = 200$ kHz/V, $R = 500\ \Omega$, and $C = 100$ nF. The plasma frequency $\omega_p/2\pi$ was adjusted to 9.4 kHz ($I_{dc} = 0.6$ mA) and L_0 was chosen to give $\omega_R/2\pi = 25$ kHz. The analog experiment proceeded in the following way. The two resonance frequencies ω_1 ($\approx \omega_p$) and ω_2 ($\approx \omega_R$) were measured in the small-signal limit; a pump signal was applied at the frequency $\omega_1 + \omega_2$ and the amplitude was gradually increased while the voltage waveform was observed on an oscilloscope. At a certain threshold pump voltage V_{rf}^{crit}, the voltage waveform suddenly changed and the frequencies ω_1 and ω_2 appeared with large amplitude as seen in Fig. 2(b). Figure 2(a) shows the voltage waveform just below the threshold rf voltage, it contains only the pump frequency (and some higher harmonics). Figure 3 shows the quantity $\alpha_c = kV_{rf}^{crit}/f_{pump}$ as a function of the pump frequency. Curve (a) of Fig. 3 shows the threshold curve for the nondegenerate parametric excitation when pumped with a frequency in the vicinity of $\omega_p + \omega_R$ and curve (b) of Fig. 3 shows the threshold curve for the singly degenerate parametric excitation when the pump frequency is twice the plasma frequency.[6] Taking the total circuit losses into account, the threshold values of Fig. 3 are in agreement with the derived ones [Eqs. (16) and (18)] within the experimental uncertainty.

In addition, different types of frequency conversion were investigated. The voltage components at the different frequencies were measured by means of a spectrum analyzer. For example if one rf biased the analog just below the threshold curve at a frequency $\omega_p + \omega_R$ and applied a small signal at ω_p, an amplified signal at ω_R could be observed in general agreement with the Manley–Rowe relations.[11]

IV. POSSIBILITIES FOR A REAL JUNCTION EXPERIMENT

Both the singly and doubly degenerate parametric modes have recently been observed experimentally.[8–10] Here we discuss, at least qualitatively, the possibilities for an experiment on the nondegenerate parametric mode. The approximative model assumed in Sec. II is a too simplified model for the situation in a real junction. In a real junction the plasma mode and the geometrical mode have different electromagnetic field configurations and, hence, a lumped circuit model as in Fig. 1 is insufficient. However, the important requirement for the theory to hold is that a coupling between the plasma mode and the geometrical mode exists. Theoretically, this coupling could be calculated by setting up Maxwell's equations and calculating the spatial overlap between the two modes. However, this would require a computer calculation based on a distributed junction model. Experimentally, only in plasma resonance experiments[17] such a coupling has been reported.

That a coupling between the plasma mode and the geometrical mode exists may be understood from simple intuitive arguments.

The plasma mode is assumed to have a uniform longitudinal (i.e., transverse to the barrier) electric field. The geometrical mode has a spatially varying longitudinal component of the electric field. For the odd modes the electric field at the two junction edges point in opposite directions. For the even modes, however, the electric field at the two edges point in the same direction. Thus these modes have a spatial overlap (depending on the standing wave ratio) to the uniform plasma mode and seems more favorable for a coupling. These qualitative arguments may be further supported by comparison to the so-called self-induced steps.[18] In this case the (spatially uniform) electric field due to the Josephson voltage couples to the even geometrical modes. In any case, the spatial overlap and, hence, the coupling may be improved by an applied dc magnetic field, since the spatial variation of the plasma mode electric field is magnetic field dependent, whereas the geometrical mode field configuration is not.

Finally, by controlled fabrication of a tunnel junction, ω_p and ω_R may be chosen independently since they depend partly on different junction parameters.

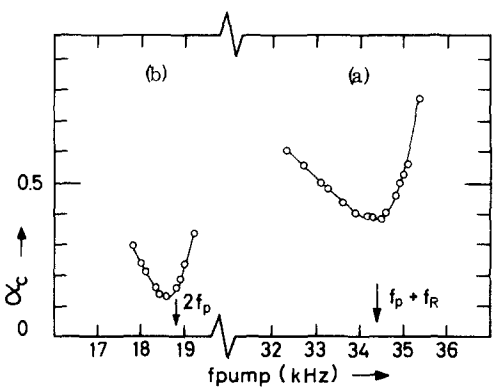

FIG. 3. Threshold curves for (a) the nondegenerate mode and (b) the singly degenerate mode, as a function of the pump frequency. $f_p = 9.4$ kHz and $f_R = 25$ kHz. Ordinate: $\alpha_c = kV_{rf}^{crit}/f_{pump}$. Circuit parameters are in the text.

V. CONCLUSION

A nondegenerate parametric element (lower sideband up-converter), using the junction plasma resonance and the junction geometrical resonance as signal and idler circuits, respectively, has been suggested. The element has been investigated by means of a Josephson junction analog, and agreement between the calculations and the analog results was found.

ACKNOWLEDGMENT

Stimulating discussions with M.R. Samuelsen, O. Hoffmann Soerensen, C.K. Bak, E. Kollberg, and O. Nilsson are gratefully acknowledged.

[1]P. Russer, Arch. Elektrischen Übertragung **23**, 417 (1969).
[2]H. Kanter and A.H. Silver, Appl. Phys. Lett. **19**, 515 (1971).
[3]H. Zimmer, Appl. Phys. Lett. **10**, 193 (1967).
[4]A.N. Vystavkin, V.N. Gubankov, G.F. Leschenko, K.K. Likharev, and V.V. Migulin, Radio Eng. Electron. Phys. **15**, 2121 (1970).
[5]A.N. Vystavkin, V.N. Gubankov, L.S. Kuzmin, K.K. Likharev, V.V. Migulin, and V.K. Semenov, Rev. Phys. Appl. **9**, 79 (1974).
[6]N.F. Pedersen, M.R. Samuelsen, and K. Saermark, J. Appl. Phys. **44**, 5120 (1973).
[7]P.T. Parrish, M.J. Feldman, H. Ohta, and R.Y. Chiao, Rev. Phys. Appl. **9**, 229 (1974).
[8]C.K. Bak, B. Kofoed, N.F. Pedersen, and K. Saermark, Proceedings of the applied Superconductivity Conference, 1974, Oakbrook, Ill. (unpublished); J. Appl. Phys. **46**, 886 (1975).
[9]A.J. Dahm and D.N. Langenberg, J. Low Temp. Phys. (to be published).
[10]P.T. Parrish and R.Y. Chiao, Appl. Phys. Lett. **25**, 627 (1974).
[11]P. Pennfield and R.P. Rafuse, *Varactor Applications* (MIT Press, Cambridge, Mass., 1962).
[12]O.H. Soerensen, T.F. Finnegan, and N.F. Pedersen, Appl. Phys. Lett. **22**, 129 (1973).
[13]If the junction is considered ac-current driven, harmonics of ω_{pump}, ω_1 and ω_2 will appear in the voltage. These frequency components may be retained in the calculations (Ref. 11). However, unless the junction has a resonance at one of these frequencies only minor quantitative changes will occur in the first-order calculations discussed here.
[14]M. Abramowitz and I.A. Stegun, *Handbook of Mathematical Functions* (Dover, New York, 1965).
[15]The substitutions are $C(t) \rightarrow 1/L(t)$, $r \rightarrow 1/R$: and $V \rightarrow I$.
[16]C.K. Bak and N.F. Pedersen, Appl. Phys. Lett. **22**, 149 (1973).
[17]N.F. Pedersen, T.F. Finnegan, and D.N. Langenberg, *Proceedings of the Thirteenth International Conference on Low Temperature Physics* (Plenum, New York, 1974), Vol. III, p. 268; Phys. Rev. B **6**, 4151 (1972).
[18]C.T. Chen and D.N. Langenberg, *Proceedings of the Thirteenth International Conference on Low Temperature Physics* (Plenum, New York, 1974), Vol. III, p. 289.